ChemComm

COMMUNICATION

View Article Online
View Journal | View Issue

Cite this: *Chem. Commun.*, 2025, **61**, 11625

Received 8th May 2025,
Accepted 23rd June 2025

DOI: 10.1039/d5cc02215k

rsc.li/chemcomm

Backbone cleavage of peptides and proteins *via* cysteine *S*-fluoroacetylation†

Yuya Matsumoto, Naoki Zenmyo, Shunsuke Watanabe, Kaori Sasaki-Tabata, Shohei Uchinomiya, Naoya Shindo and Akio Ojida *

***S*-Fluoroacetylation of cysteine residues enables efficient cleavage of main-chain amide bonds in peptides and proteins under neutral aqueous conditions.**

In biological systems, cleavage of protein amide backbones is a key post-translational modification that modulates protein function.[1,2] In contrast, chemical methods for site-selective protein cleavage remain underdeveloped, despite their potential for artificially regulating protein functions. This is mainly because of the limited availability of biocompatible chemical reactions.[3–9] We recently developed a protein cleavage platform based on cysteine formylation, which promotes hydrolysis of the adjacent amide bond under neutral aqueous conditions, enabling site-selective cleavage.[10] However, this approach was limited by the narrow range of acylating reagents tested. In the present study, we aimed to identify new cysteine acylation reactions to expand the scope of protein cleavage chemistry. We found that cysteine acylation with a fluoroacetyl group effectively induces amide bond cleavage in peptides and proteins. Notably, fluoroacetylation showed higher cleavage efficiency than formylation, depending on the amino acid sequence, highlighting its potential as a new chemical tool for selective protein cleavage.

In our previous study, we proposed that cysteine acylation with small, strongly electron-withdrawing acyl groups, such as formyl, would effectively induce protein cleavage.[10] Building on this concept, we investigated α-haloacetyl groups, which meet these criteria. The calculated pK_a values of halo-substituted carboxylic acids[11] suggest that haloacetyl groups have stronger electrophilicity than acetyl groups, making them promising candidates for cysteine acylation (Table S1, ESI†). Therefore, we synthesised reagents **1–5** with different acyl groups (Fig. 1a). Reagents **1–5** were designed based on an *N*-sulfonyl amino acid scaffold.[12,13] We anticipated that introducing different substituents at the α-carbon of the amino acid and the sulfoamide moieties would allow fine-tuning of their electrophilic reactivity. Initial screening was conducted using peptide-**a**, designed to restore the fluorescence of 7-hydroxycoumarin upon cleavage of a 2,4-dinitrophenyl quencher group (Fig. 1b and Fig. S1, ESI†). Time-dependent fluorescence analysis showed that fluoroacetylation reagent **1** induced the greatest fluorescence recovery under neutral aqueous conditions (100 mM phosphate buffer containing 30% MeCN, pH 7.4, 37 °C; Fig. 1c). Liquid chromatography-mass spectrometry (LC-MS) analysis revealed the rapid formation of *S*-fluoroacetylated peptide-**a**, followed by the formation of the N-terminal fragment ($[M + H]^+$ = 491.19) and C-fragments ($[M + H]^+$ = 512.16) after 24 h (Fig. 1d). Reagents **2–5** induced slower cleavage, with fragment yields less than half of those from reagent **1** after 24 h. The lower cleavage efficiency of difluoroacetyl reagent **2** was likely due to its low aqueous stability ($t_{1/2}$ < 1 h) under neutral aqueous conditions.

Next, we modulated the electrophilic reactivity of the fluoroacetylation reagent **1** to achieve selective acylation of the target cysteine residues. Reagent **1** exhibited high reactivity toward cysteine derivatives such as glutathione (GSH) ($t_{1/2}$ = 0.38 h; Table 1) and was prone to hydrolysis ($t_{1/2}$ = 1.38 h) under neutral aqueous conditions (pH 7.4, 37 °C). The high electrophilic reactivity of **1** was effectively reduced by introducing an alkyl group at the α-position of the amino acid moiety (*e.g.*, reagents **6** and **7**). Additionally, introducing a bulky alkyl group on the sulfonamide moiety (*e.g.*, reagents **8** and **9**) further reduced the electrophilic reactivity of reagent **1**. These results highlight the versatility of the *N*-sulfonyl amino acid scaffold for tuning electrophilicity in the design of fluoroacetylation reagents. The half-lives of the reagents in the presence of *N*-acetyl-Lys were comparable to their aqueous stabilities, suggesting low reactivity toward lysine residues under neutral aqueous conditions. Among the tested reagents, we selected reagent **6** for subsequent protein/peptide cleavage experiments because of its high GSH reactivity ($t_{1/2}$ = 0.66 h) and sufficient

Graduate School of Pharmaceutical Sciences, Kyushu University, 3-1-1 Maidashi, Higashi-ku, Fukuoka 812-8582, Japan. E-mail: ojida@phar.kyushu-u.ac.jp

† Electronic supplementary information (ESI) available. See DOI: https://doi.org/10.1039/d5cc02215k

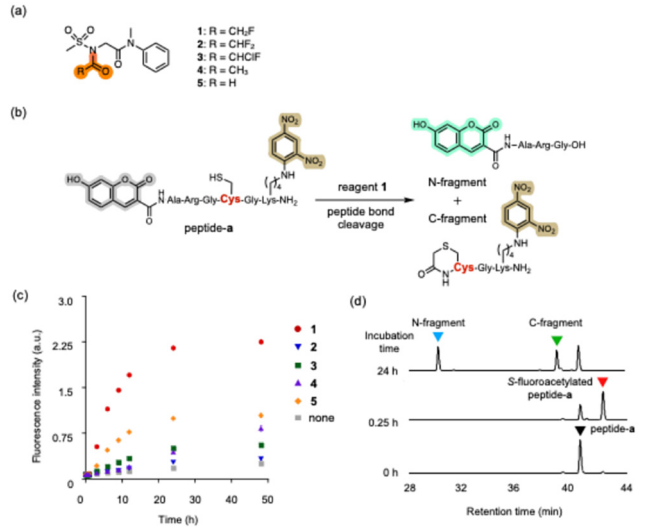

Fig. 1 Peptide bond cleavage induced by cysteine *S*-acylation. (a) Chemical structures of the sulfonamide-based acylation reagents. (b) Peptide bond cleavage of peptide-**a** through cysteine modification. (c) Time plot of the fluorescence changes of peptide-**a** (15 μM) upon treatment with acylation reagents **1–5** (1 mM). Reaction conditions: 100 mM sodium phosphate buffer (pH 7.4), 30% MeCN, 0.3 mM TCEP, 37 °C. $\lambda_{ex}/\lambda_{em}$ = 400/450 nm. Data are expressed as the mean ± SD of three independent experiments. (d) HPLC analysis of the cleavage reaction of peptide-**a** by *S*-fluoroacetylation. Peptide-**a** (10 μM) was treated with reagent **1** (5 mM) in 100 mM sodium phosphate buffer (pH 7.4) containing 10% DMF in the presence of 0.3 mM TCEP at 37 °C. The peaks were detected by UV absorbance at 370 nm. The peptides were identified by ESI-TOF-MS analysis. The structure of the cyclized C-fragment is shown in Fig. 2c.

Table 1 Summary of the aqueous stability and electrophilic reactivity of *N*-fluoroacetyl sulfonamides[a]

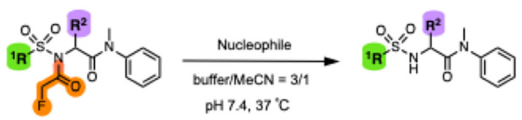

Compound	Substituent R^1	Substituent R^2	Nucleophile: $t_{1/2}$ (h) GSH	*N*-Ac-Lys	None
1	Me	H	0.38	1.43	1.38
6	Me	Me	0.66	7.01	6.57
7	Me	iPr	1.21	21.3	22.2
8	iPr	Me	4.15	31.5	43.5
9	*t*Bu	Me	28.2	29.4	38.3

[a] Data represent the average of triplicate experiments.

aqueous stability ($t_{1/2}$ = 6.57 h). The reaction selectivity of **6** was further evaluated using a small ubiquitin protein (8.6 kDa), which possesses seven lysines but lacks cysteine on the surface. The MALDI-TOF mass analysis revealed that the treatment of ubiquitin (4 μM) with **6** (1 or 5 mM) resulted in the partial mono-fluoroacetylation after 72 h (Fig. S2, ESI†). We speculated that this mono-fluoroacetylation occurs at K48, which is highly reactive and susceptible to acylation, as reported in our previous paper.[10]

We investigated the reaction mechanism of fluoroacetylation-induced peptide cleavage using LC-MS (Fig. 2b and c). Treatment of peptide-**a** with reagent **6** led to the rapid formation of *S*-fluoroacetylated peptide-**a1** ($[M + H]^+$ = 1004.33) within 0.25 h, which gradually changed to a new peak corresponding to peptide-**a2** after 6 h. Peptide-**a2** showed the same *m*/*z* value as peptide-**a1**, suggesting they are the structural isomers. We hypothesised that peptide-**a2** is a thioester intermediate formed *via* intramolecular acyl transfer from peptide-**a1**. This hypothesis aligns with the mechanism of cysteine acetylation-induced peptide bond cleavage recently proposed by Gless *et al.*[14] The thioester intermediate (peptide-**a2**) subsequently underwent hydrolysis to generate the N-terminal fragment ($[M + H]^+$ = 491.19), while the cleaved C-fragment cyclized intramolecularly to yield a cyclic product ($[M + H]^+$ = 512.16). We also observed an *S*-fluoroacetylated C-fragment ($[M + Na]^+$ = 614.15), which was hydrolysed to revert to the C-fragment. The cleavage reaction was nearly complete within 24 h, which was consistent with the results of fluorescence monitoring of the cleavage reaction (Fig. 1c). LC-MS analysis also indicated that *S*-fluoroacetylated peptide-**a1** remained stable for several hours under neutral aqueous conditions. ^{1}H-NMR analysis showed that the *S*-fluoroacetylated cysteine analogue **10** had a half-life ($t_{1/2}$) of 23.5 h in aqueous buffer (Fig. S3–S5, ESI†), which is approximately four times longer than that of *S*-formylated cysteine **11** ($t_{1/2}$ = 6.2 h) (Fig. S2, ESI†). In contrast, *S*-acetylated cysteine **12** was stable for over 24 h without hydrolysis. These findings suggest that *S*-fluoroacetylated species have higher electrophilicity than their *S*-acetylated counterparts, while maintaining sufficient aqueous stability. This balance facilitates intramolecular acyl transfer and promotes efficient peptide bond cleavage.

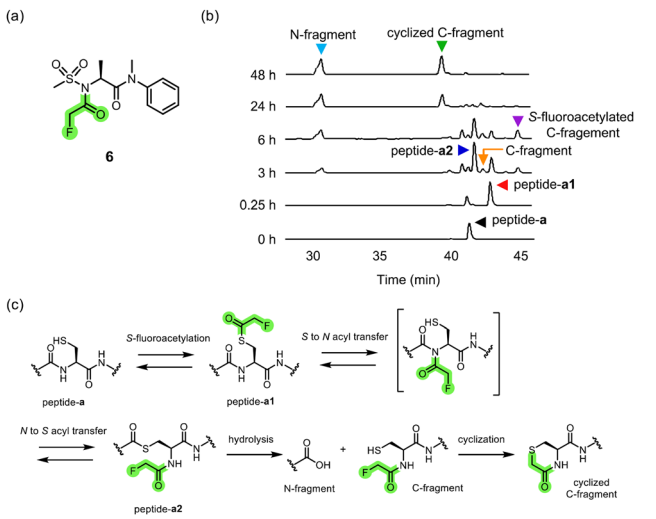

Fig. 2 HPLC analysis of peptide-a cleavage by cysteine *S*-fluoroacetylation. (a) Chemical structure of *S*-fluoroacetylation reagent **6**. (b) HPLC analysis of the cleavage reaction of peptide-**a** by *S*-fluoroacetylation. Peptide-**a** (10 μM) was treated with **6** (5 mM) in 100 mM sodium phosphate buffer (pH 7.4) containing 10% DMF in the presence of 0.3 mM TCEP at 37 °C. The peaks were detected by UV absorbance at 370 nm. The peptides were identified by ESI-TOF-MS analysis. (c) Proposed reaction mechanism of peptide bond cleavage induced by *S*-fluoroacetylation.

We evaluated the sequence dependency of peptide bond cleavage induced by *S*-fluoroacetylation using reagent **6**. The initial reaction rates (ΔF/h) for various peptides are summarised in Fig. 3 and Fig. S6 (ESI†). The results showed that peptide-**a**, **b**, **c**, and **d**, possessing Gly, Arg, Asn, His at the adjacent Xaa position, respectively, exhibited the same level of high reaction efficiency (Fig. 3b and Fig. S7, ESI†). Conversely, amino acids with a bulky hydrophobic side chain, such as Tyr, Leu, Pro, Trp, Val, and Ile, at Xaa position greatly decelerated the cleavage reactions. The peptides with other nine amino acids have a moderate reactivity between them. It is noteworthy that **6** demonstrated a higher sequence tolerability in comparison to formylation reagent **5** (Fig. 3c and Fig. S8, ESI†), suggesting the broader utility of *S*-fluoroacetylation in the peptide cleavage. The peptides with different amino acids at the Yaa position did not cause significant changes in the reaction rate (Fig. S6, ESI†).

Next, we used *S*-fluoroacetylation to cleave the protein backbones. We initially employed maltose binding proteins (MBP) possessing a single cysteine residue in the Gly-Cys-Asp8 peptide tag at the C-terminus (Fig. 4a). Treatment of the tag-fused MBP-GC with reagent **6** (1 or 5 mM) resulted in the formation of truncated proteins at the tag site, as confirmed by SDS-PAGE and MALDI-TOF mass spectrometry (Fig. 4b–d). We next attempted to cleave MBPs carrying single cysteine point mutations (I34C, D56C, and I267C). I34C and D56C are in flexible loop regions, whereas I267C is in the C-terminus of a β-sheet. All three residues are surface-exposed and accessible to reagent **6**. SDS-PAGE and MALDI-TOF mass analyses revealed partial cleavage at these cysteine sites upon treatment with **6** (Fig. 4e and Fig. S9, ESI†). The lower cleavage efficiency at these internal cysteine sites might be due to their more rigid structure compared to the C-terminus of MBP-GC. Treatment of a triple cysteine mutant MBP (I34C/D56C/I267C) with reagent **6** resulted in near-complete disappearance of the full-length protein and generation of multiple cleavage fragments (Fig. 4f and Fig. S10, ESI†). Notably, reagent **6** exhibited a higher cleavage efficiency than formylation reagent **5**.

In conclusion, we demonstrated that fluoroacetylation of cysteine residues effectively induces site-selective backbone cleavage of peptides and proteins. This method offers distinct advantages, including higher cleavage efficiency compared to cysteine acetylation[14] and a unique sequence selectivity profile that differs from cysteine formylation. These features establish

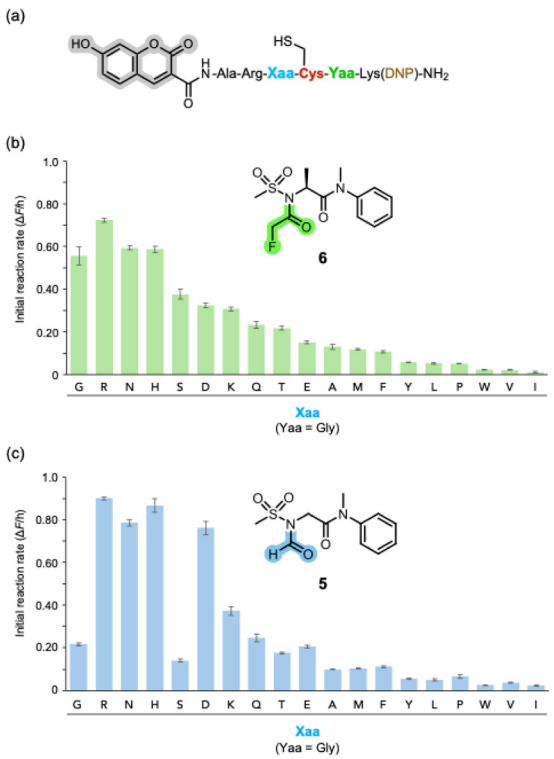

Fig. 3 Sequence dependence of the peptide cleavage reaction induced by cysteine *S*-acylation. (a) Peptide structure with different amino acids at Xaa position. (b) and (c) Initial reaction rates (0–3 h) of the peptide cleavage reaction (ΔF/h) upon treatment with reagents **6** and **5**. Reactions were conducted with the peptide (15 μM) and the reagent (1 mM) in 100 mM sodium phosphate buffer (pH 7.4) containing 30% MeCN in the presence of 0.3 mM TCEP at 37 °C. $\lambda_{ex}/\lambda_{em}$: 400/450 nm. Data are expressed as the mean ± SD of three independent experiments.

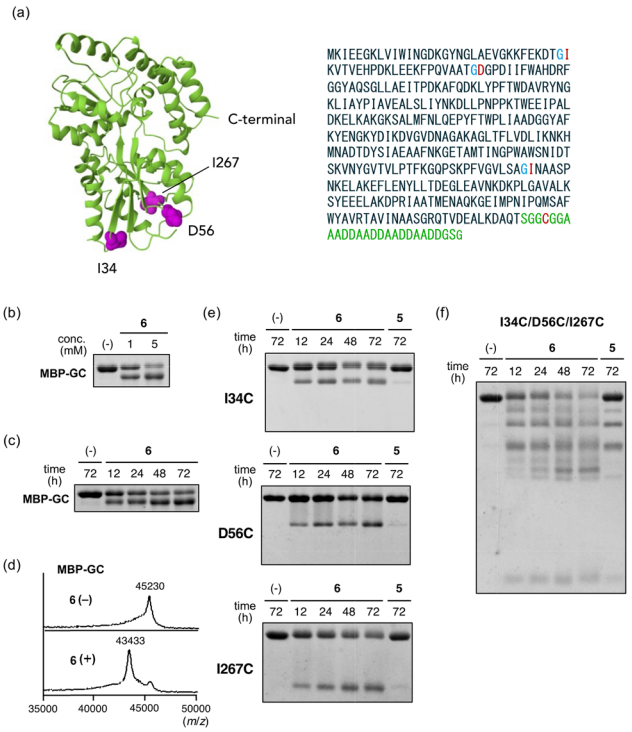

Fig. 4 Protein cleavage induced by cysteine *S*-fluoroacetylation. (a) Crystal structure and amino acid sequence of MBP1-367 (PDB: 1ANF), with mutated cysteine sites highlighted in magenta. A peptide tag containing a cysteine residue is fused to the C-terminus. (b) and (c) Cleavage of tag-fused MBP-GC using reagent **6**. MBP-GC (4 μM) was treated with the reagent in 100 mM sodium phosphate buffer (pH 7.4) containing 30% MeCN in the presence of 5 mM TCEP at 37 °C. (b) Incubation time was 72 h. (c) The concentration of reagent **6** was 5 mM. The proteins and the fragments were detected using protein-binding fluorescent dyes. (d) MALDI-TOF-MS analysis of the cleavage of tag-fused MBP using reagent **6**. (e) and (f) Cleavage of point-mutated MBP (4 μM) using **6** and **5** (5 mM). MBP (4 μM) was treated with the reagent in 100 mM sodium phosphate buffer (pH 7.4) containing 30% MeCN in the presence of 5 mM TCEP at 37 °C.

fluoroacetylation as a new and versatile platform for peptide and protein cleavage. Furthermore, we successfully developed *N*-sulfonyl α-amino acids as a new class of reagents for cysteine fluoroacetylation. We expect that their flexible structural modification and tunable electrophilicity will provide a superior reagent with better amino acid selectivity and improved protein cleavage efficiency. We also anticipate that these improvements will facilitate future application of this cleavage platform for target- and site-selective peptide and protein manipulation.

This work was supported by Grant-in-Aid for Challenging Exploratory Research (JSPS KAKENHI Grant No. 20K21254 to AO), Grant-in-Aid for Scientific Research B (JSPS KAKENHI Grant No. 23H02085 to AO), Core Research for Evolutional Science and Technology (CREST) (JST, Grant No. JPMJCR24T1 to AO), Grant-in-Aid for Specially Promoted Research (JSPS KAKENHI Grant No. 23H05405 to AO and NS) and JST SPRING (JST, Grant No. JPMJSP2136 to YM.).

Conflicts of interest

The authors declare no competing financial interest.

Data availability

Details of the experimental procedures and NMR spectra are available in the ESI.† The uncropped raw images of all electrophoresis data are available free of charge at **https://doi.org/10.7910/DVN/I8IBAA** (Harvard Dataverse, V2).

Notes and references

1 C. T. Walsh, S. Garneau-Tsodikova and G. J. Gatto, Jr, *Angew. Chem., Int. Ed.*, 2005, **44**, 7342–7372.
2 H. Paulus, *Annu. Rev. Biochem.*, 2000, **69**, 447–496.
3 H. Y. Tang and D. W. Speicher, *Anal. Biochem.*, 2004, **334**, 48–61.
4 J. Wu and J. T. Watson, *Anal. Biochem.*, 1998, **258**, 268–276.
5 Y. Seki, K. Tanabe, D. Sasaki, Y. Sohma, K. Oisaki and M. Kanai, *Angew. Chem., Int. Ed.*, 2014, **53**, 6501–6505.
6 B. Dang, B. Dang, M. Mravic, H. Hu, N. Schmidt, B. Mensa and W. F. DeGrado, *Nat. Methods*, 2019, **16**, 319.
7 T. A. Mollner, T. A. Mollner, A. M. Giltrap, Y. Zeng, Y. Demyanenko, C. Buchanan, D. Oehlrich, A. J. Baldwin, D. C. Anthony, S. Mohammed and B. G. Davis, *Sci. Adv.*, 2022, **8**, eabl8675.
8 S. Zhang, L. M. D. L. Rodriguez, F. F. Li, R. Huang, I. K. H. Leung, P. W. R. Harris and M. A. Brimble, *Chem. Sci.*, 2022, **13**, 2753–2763.
9 M. Jbara, E. Eid and A. Brik, *J. Am. Chem. Soc.*, 2020, **142**, 8203–8210.
10 N. Zenmyo, Y. Matsumoto, A. Yasuda, S. Uchinomiya, N. Shindo, K. Sasaki-Tabata, E. Mishiro-Sato, T. Tamura, I. Hamachi and A. Ojida, *J. Am. Chem. Soc.*, 2025, **147**, 3080–3091.
11 *Calculated using Advanced Chemistry Development (ACD/Labs) Software* (©1994-2025 ACD/Labs).
12 T. Tamura, T. Ueda, T. Goto, T. Tsukidate, Y. Shapira, Y. Nishikawa, A. Fujisawa and I. Hamachi, *Nat. Commun.*, 2018, **9**, 1870.
13 S. Guillard, A. Aramini, M. C. Cesta, S. Colagioia, S. Coniglio, F. Genovese, G. Nano, E. Nuzzo, V. Orlando and M. Allegretti, *Tetrahedron*, 2006, **62**, 5608–5616.
14 B. H. Gless, S. H. Schmied and C. A. Olsen, *JACS Au*, 2025, **5**, 67–72.

